




## Article

# Design and Parametric Analysis of a Solar-Driven Façade Active Layer System for Dynamic Insulation and Radiant Heating: A Renovation Solution for Residential Buildings

Emmanouil Katsigiannis , Petros Antonios Gerogiannis, Ioannis Atsonios, Ioannis Mandilaras \*   
and Maria Founti 

Laboratory of Heterogeneous Mixtures and Combustion Systems, School of Mechanical Engineering, National Technical University of Athens, Heron Polytechniou 9, Zografou, 15780 Athens, Greece; makatsigiannis@mail.ntua.gr (E.K.); petrosgerogiannis7@gmail.com (P.A.G.); atsoniosgiannis@central.ntua.gr (I.A.); mfou@central.ntua.gr (M.F.)

\* Correspondence: giannis.mandilaras@gmail.com

**Abstract:** The constantly increasing energy demand in aged households of urban areas highlights the need for effective renovation solutions towards nZEB to meet the European Commission's energy reduction and decarbonization targets. To address these targets, a variety of retrofitting interventions are proposed that incorporate hydronic systems into the building envelope, minimizing heat loss through the external walls and occasionally heating or cooling adjacent thermal zones. The present study analyses a low-temperature solar-powered hydronic active wall layer attached to the skin of a residential building in combination with solar collectors for heat generation. A typical floor of a five-storey, post-war, poorly insulated multi-family building is modelled considering two different climatic conditions: Berlin (Germany) and Kastoria (Greece). The design parameters, such as the area of the collector, the temperature of the fluid entering the active layer, the volume of the buffer tank and insulation thickness have been determined in order to optimize the impact on the heating system. Techno-economic assessment—followed by sensitivity analysis—has been conducted to scrutinize the feasibility of such a renovation solution. Last but not least, the nZEB compliance for both cases is examined based on EU and national nZEB definitions. The results indicate that a reduction of heating demand by up to 93% can be achieved, highlighting that such a renovation solution can be profitable in both examined locations while at the same time reaching the nZEB state.

**Keywords:** thermal active layer; active insulation; façade-integrated hydronic system; TRNSYS modelling; techno-economic study; parametric analysis; nZEB renovation



**Citation:** Katsigiannis, E.; Gerogiannis, P.A.; Atsonios, I.; Mandilaras, I.; Founti, M. Design and Parametric Analysis of a Solar-Driven Façade Active Layer System for Dynamic Insulation and Radiant Heating: A Renovation Solution for Residential Buildings. *Energies* **2023**, *16*, 5134. <https://doi.org/10.3390/en16135134>

Academic Editor: Carla Montagud

Received: 26 April 2023

Revised: 13 June 2023

Accepted: 26 June 2023

Published: 3 July 2023



**Copyright:** © 2023 by the authors. Licensee MDPI, Basel, Switzerland. This article is an open access article distributed under the terms and conditions of the Creative Commons Attribution (CC BY) license (<https://creativecommons.org/licenses/by/4.0/>).

## 1. Introduction

Towards achieving an nZEB state, buildings should demonstrate very high energy performance, where the near-zero or very low amount of energy required should be covered as much as possible by renewable energy sources produced on-site or nearby [1]. This requires an effective protective building envelope that prevents heat transmission and maintains indoor thermal comfort in a more efficient way [2–7]. A promising technology in terms of building energy efficiency is the embedded radiant system, which is a piping (or other) network incorporated into the components of the building's envelope. Various radiant or active systems integrated into the building façade have been explored and developed in this regard [8].

Based on ISO, European (EN) and AHSRAE standards, three main types of such systems can be identified: (1) hydronic radiant panels, where pipes are attached to metal panels by means of hangers [9,10]; (2) embedded surface systems (ESSs), where the pipes are embedded in the surface of the slab/wall but are insulated from the structure;

and (3), thermally activated building systems (TABS), where the pipes are embedded in a massive concrete slab/mass (within the structure) [11].

Focusing on the third type, the activated envelope surfaces mainly exchange heat with the room in the form of radiation and consequently exchange heat directly with the occupants. This attribute provides both comfort and energy advantages. Thermal comfort is favored since heating and cooling with TABS minimize the required air change rate for ventilation. Therefore, draughts and noise are reduced. Regarding energy, an operative temperature inside the comfort range can be maintained with variable air temperature, consequently reducing ventilation energy loss as the indoor air has a temperature nearer to the outdoor air temperature [12].

Even though radiant or active heating and cooling systems have been traditionally considered part of structural floors or ceilings, there is much evidence that active walls can also provide feasible solutions [8,13–15]. Compared to floor or ceiling systems, a crucial advantage, *inter alia*, is that these walls operate as thermal barriers to decrease heating and cooling loads. This is accomplished by adjusting the water temperature to a value that does not necessarily lead to space heating or cooling but reduces heat transmission through the walls [8,16–18].

Additionally, in combination with the wall's thermal mass, there is an important flexibility potential in terms of energy storage capacity. Such capacity could allow for a reduction in peak heating or cooling power by shifting the peak load to periods in which the system works at low capacity; namely, to "reallocate" an amount of the demand to periods in which the system is less busy and could operate more efficiently [12].

Considering the operation of active walls, two categories can be observed most commonly depending on the temperature of the circulating water and the configuration of the wall layers and the piping network: systems that operate as a building's thermal barrier and radiant or active walls, which are partially or entirely used for space heating/cooling [8,16]. However, even for the systems that are used for space heating, it is possible to occasionally circulate water with low-grade temperatures, and they are therefore used as thermal barriers. From the conclusions of the study in [16], the alternation from thermal barrier to space heating operation and vice versa is achieved by actively controlling the temperature of the supply water depending on the current conditions and the system's configuration.

Thermal barriers are used as passive–active systems with the ability to differentiate the thermal transmittance of the external wall and modulate the temperature difference between outdoor and indoor environments [16,19,20]. Yu et al. proposed a thermo-activated wall with an embedded mini-tube capillary network, which circulates water at temperatures close to ambient, indicating that such systems can potentially counterbalance the thermal load or indirectly heat/cool the indoor space [21]. Another approach explored in [22,23] introduces the use of embedded closed-loop pipes in the external walls, which utilize solar gains by transferring solar-heated water from southern surfaces to walls with a north orientation. Consequently, this heat redistribution decreased the heat losses more significantly during winter and summer, yet it proved less efficient in more severe climates [17,22,23].

A patent worth mentioning relates to an active insulation system relating to the energy performance of an experimental residence located in a heating-intensive town in Hungary, where a wall-integrated piping network had been coupled with a ground heat exchanger. Based on the conclusions of this work, for a water temperature range of 14–25 °C, the annual heat losses were reduced by 63% on average compared to standard insulation [24]. Another experimental validation of an active pipe-embedded building envelope is described in [25]. This work showed that the introduced semi-dynamic simplified model can adequately predict the semi-steady or pure dynamic thermal performance of the examined wall-integrated system by comparing it with the corresponding measurements.

Furthermore, envelope-integrated hydronics (i.e., systems achieving heating or cooling via the heat transfer of a circulating fluid) in combination with the external wall's thermal mass provide increased exploitable thermal inertia for use in potential demand shifting. A radiant wall heating system embedded in a heavy brick construction and coupled with

a ground source heat pump supplied was experimentally tested under real conditions in [12]. The results showed that not only is there a potential saving between 20 and 40% based on the temperature set-point, but most importantly, that the active thermal mass enabled peak load shifting. In the work of [26], the cooling energy performance of an active insulation system combined with a thermally activated storage system is examined. Similarly, the objective is to store energy during non-peak load hours or when using renewable sources such as solar radiation and provide heating and cooling during the peak hours of occupancy. It is worth mentioning the results presented in [27–31], which also highlight the importance of controlling thermally active walls and the subsequent contribution to peak load shifting [8,11,15,21–24,32–36].

Last but not least, Keshanarzzadeh et al. prepared and assessed a comprehensive dynamic model of a renewable-based system combining cooling, heating and power abilities (CCHP) [37]. This system incorporates parabolic trough solar collectors (PTSCs) and an organic Rankine cycle with an absorption chiller and proton exchange membrane electrolyzer. The examined system is analyzed using a multi-objective optimization method to determine the optimal design parameters of the CCHP system and demonstrate the optimized case on a Pareto curve.

Most previous works focused on system evaluation and the resulting energy performance benefits without a detailed analysis of the techno-economic aspects. The aim of the current study is to present and assess the energy and the techno-economic performance of a solar-powered active layer system that is supplied by water heated from solar gains via a thermal collector.

A parametric study is conducted aiming to determine the impact of crucial operational parameters, such as the inlet temperature, the area of the solar collector, the volume of the buffer tank and the additional insulation thickness, on the building's energy performance and economic viability. Additionally, the analysis evaluates the techno-economic aspect of the designed systems to present their feasibility/profitability in renovation scenarios.

A case study of a typical storey of a multi-family building is used for the energy and techno-economic assessment. The application of the active layer system to this part of the residential building is conducted aiming to quantify the potential energy savings and scrutinise the contribution of such a system towards achieving an nZEB state.

Furthermore, the work examines the system's suitability under diverse climates with significantly different cold periods and available solar radiation. For this purpose, two locations are considered in this assessment: Kastoria (Greece) and Berlin (Germany).

## 2. System Overview

### *Active Layer Description*

The examined system is a vertical wall layer with embedded water-filled pipes that operates where each assigned external wall part is thermally activated. It consists of a piping grid layer, which is positioned between the external insulation and the existing masonry. This water circuit is supplied by solar thermal panels and a buffer tank for surplus heat storage. The closed-loop water circuit harvests heat directly through the solar collector (Figure 1). Since solar radiation is the exclusive heating source, the role of the solar collector is vital. Depending on the examined location and the availability of total solar radiation, the type of solar collector, as well as the combination with the buffer tank, may differ. In Mediterranean climates with long periods of solar radiation, simple selective collectors can be suitable. In central and northern European regions, where solar impact is restricted, evacuated-tube collectors are preferable. In any case, the examined active layer set up is not supported by any other heat source (a boiler or a heat pump); therefore, it would not be feasible to independently cover the entire heating demand of a household.

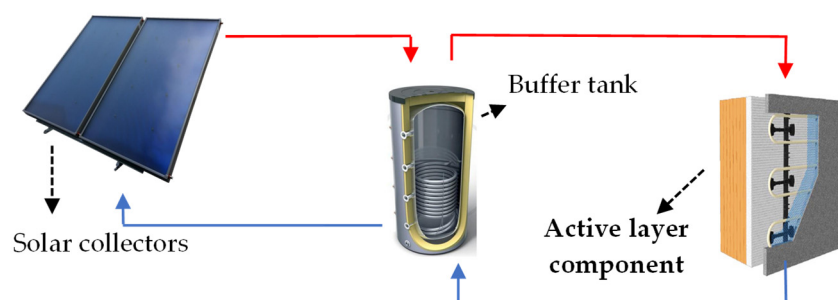


**Figure 1.** Active layer system overview.

By circulating water into the active layer with the assistance of an electrical pump, a temperature condition is imposed, creating a thermal barrier and resulting in heat loss reduction. Depending on the temperature of the inlet water and the indoor/outdoor conditions, the thermal barrier can alternate its operation to space heating. If the temperature setpoint of the water entering the envelope is above 25 °C, the external wall operates as a radiant heating terminal. This setpoint limitation may vary as it is mostly dependent on the preferred indoor temperature conditions.

### 3. Methodology

This section starts with a description of the TRNSYS model used, followed by the buildings used as a case study. The framework of the parametric study is described together with the examined design parameters, the boundary conditions and the relevant cost-related assumptions. The parametric results have been evaluated with respect to energy and techno-economic indicators, which are also described. Last but not least, the nZEB compliance limit for both the German and Greek case is examined.

#### 3.1. Active Layer System Model

- The active layer is modelled using TRNBuild (a TRNSYS—associated visual interface for multizone building simulation [38]) as it enables the creation of a piping layer by defining its geometrical and thermal properties. TRNBuild offers the ability to set up and simulate an active layer and assign it as part of the geometry. Subsequently, the active layer is added between the existing wall and the external insulation, whilst an additional layer of plaster is used on both sides to facilitate the cover of the piping network. The geometrical and thermal properties of the piping (i.e., Table 1) are similar to commercial radiant systems, which are most commonly used in underfloor heating. Eventually, the inlet water temperature and mass flow rate are suitably set to comply with the corresponding outputs of the supply system.

**Table 1.** Geometrical and thermal properties of the piping network.

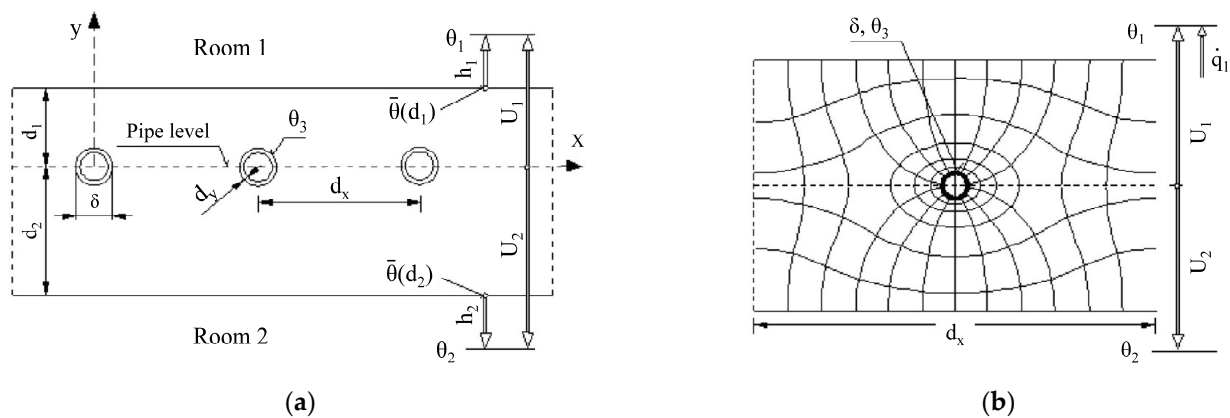
Pipe Conductivity	Pipe Spacing	Pipe outside Diameter	Pipe Thickness
0.35 W/m·K	0.1 m	17 mm	2 mm

Figure 2 depicts the structure of the active layer component inside a wall that separates two rooms: room 1 and room 2. Heat flow towards room 1 (inner space in the examined case) is calculated based on Equation (1) used by TRNSYS:

$$\dot{q}_1 = \Phi \cdot U_1 (\theta_3 - \theta_1) + (1 - \Phi) \frac{U_1 \cdot U_2}{U_1 + U_2} (\theta_2 - \theta_1) \quad (1)$$

where  $\dot{q}_1$  is the heat flow towards room 1 (Figure 2a) in  $\left[\frac{W}{m^2}\right]$ ,  $U_1$  and  $U_2$  are the heat transfer coefficient of layers between tube and room 1 and 2 in  $\left[\frac{W}{m^2 \cdot K}\right]$ , respectively,  $\theta_3$  is the temperature on the external surface of the tube in [K],  $\theta_1$  and  $\theta_2$  are the temperatures in

room 1 and 2 in [K], respectively, and  $\Phi$  is a correction factor of the thermal properties due to the piping arrangement.



**Figure 2.** Active layer description for heat flow calculation: (a) cross-section of active layer component; (b) heat flow in the cross-section of embedded tube.

The supply system is modeled using TRNSYS Simulation Studio (Figure 3). Each individual component is simulated and connected to the system using components from the software's libraries. The most significant components of the model are the following:

- Building component incorporates all parameters that were set in TRNBuild, i.e., the building's geometry and operation (occupancy, heating/cooling schedules, etc.), data concerning the structural elements (walls, roof, floor, and windows), the definition of active layer parameters, etc. A thermostat (Type2d) produces the proper signal for heating needs based on the thermal zone's temperature.
- Solar thermal collector unit (ST-Collector) is used for heat generation, exploiting solar energy to heat water. A small pump (Pump-ST) circulates the fluid taking into account the zone's heating demand and the fluid's temperature difference between the collector and the tank.
- Tank (Tank\_H) connects the source side with the load side while offering thermal storage services. The tank is also important in regulating the temperature of the supply water.
- Tempering valve control (Valve\_Heat) controls the exact mass flowrates that need to be mixed in order to achieve the desired temperature regulation based on the mixing streams. The water conditioning is achieved by mixing the hot water tank's outlet with the recirculating water exiting the active layer. This component mainly contributes to the temperature adjustment inside the active layer.

### 3.2. Case Study

The building where the examined solar-driven façade active layer system was implemented is a floor of a five-storey, post-war, poorly insulated residential building located in Germany. This part of a multi-family building is selected as a representative typology in terms of geometry and operation that can be found in several climatic conditions in Europe. The floor consists of 4 apartments, 71 m<sup>2</sup> each, and a central corridor. Each apartment is considered to be a unique thermal zone, where the interior conditions for the heating and cooling period are 20 °C and 26 °C, respectively, while the corridor is an unconditioned space. The total heat exchange surface of the envelope, which is the wall area where the examined active layer is installed, is 210 m<sup>2</sup>. The respective ratio of total heat exchange area per heated floor area is 0.74.

The building case is depicted in Figure 4, while some general building information and the obtained assumptions are summarized in Table 2. Most of the required building information, such as the construction materials, the structural elements, and their thermal properties (Tables 3 and 4), are derived from the TABULA database (Typology Approach for Building Stock Energy Assessment) [39]. The same geometry and main assumptions

are used for simulations in two different climate conditions, those of Kastoria in Greece and Berlin in Germany. Regarding the operational assumptions, steady nominal values are assumed combined with their correction factors instead of hourly schedules based on the Greek Regulation on the Energy Performance of Buildings (KENAK) [40]. The rated values of occupancy, lighting and electrical devices are presented in Table 2, and their normalization factors are 0.75, 0.1 and 0.5, respectively.

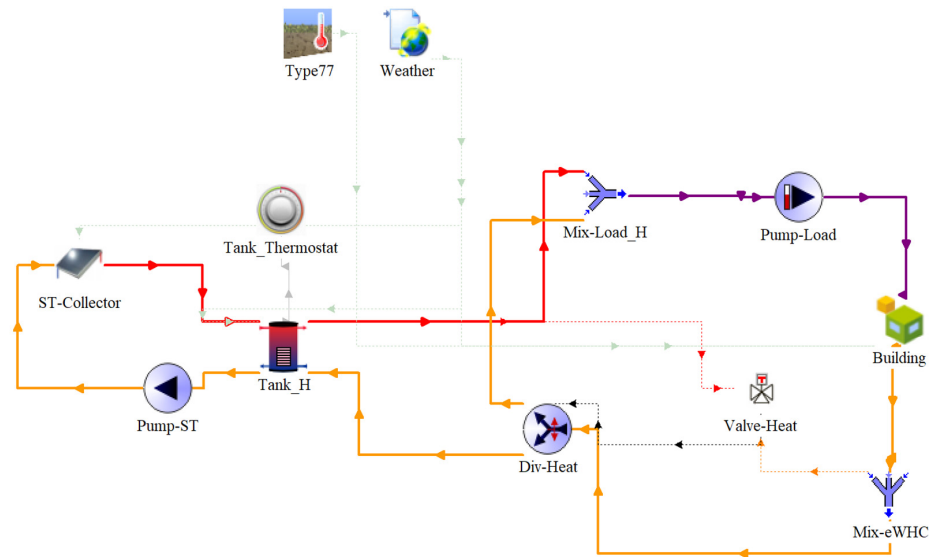


Figure 3. TRNSYS simplified model overview.

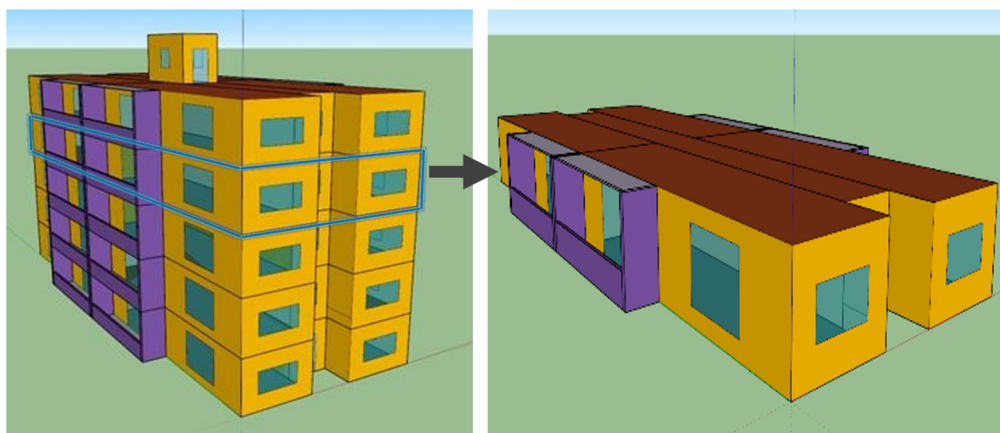


Figure 4. Building case study—geometry of examined storey.

Table 2. Building information and operational characteristics.

Description		Operation	
Type	Typical floor of five-storey multi-family building	Bearing structure	20%
Location (weather file) Apartments	Kastoria and Berlin 4	Users	0.05 p/m <sup>2</sup>
Gross Floor Area External Wall Area	282 m <sup>2</sup> 270 m <sup>2</sup>	Ventilation/Infiltration	0.25 ACH
Windows opening Area Windows to Wall Ratio	60 m <sup>2</sup> 22%	Lighting	6.4 W/m <sup>2</sup>
Gross Roof Area	17 m <sup>2</sup> /apartment	Electrical devices	4 W/m <sup>2</sup>

**Table 3.** Thermal properties of the construction materials.

Material	Conductivity (W/m·K)	Density (kg/m <sup>3</sup> )	Capacity (J/kg·K)
Concrete	1.5	1800	1000
Rendering	0.4	1500	1050
Mortar	0.87	1800	1000
Honeycomb brickwork	0.5	900	1000
Cavity blocks	0.6	1600	1100
Expanded Polystyrene (EPS)	0.033	20	1300

**Table 4.** U-values of structural elements varying with different EPS thickness.

Structural Element	U-Value (W/m <sup>2</sup> ·K)	Thickness (m)
External wall <sup>1</sup>	0.118 ÷ 1.205	0.314 ÷ 0.344
Bearing structure <sup>2</sup>	0.122 ÷ 1.827	0.314 ÷ 0.344
Internal wall	1.724	0.19
Ceiling	1.3	0.33

<sup>1</sup> The external wall's U-value varies between 1.205 W/m<sup>2</sup>·K (existing state) and 0.118 W/m<sup>2</sup>·K (250 mm of EPS);

<sup>2</sup> The bearing structure's U-value varies between 1.827 W/m<sup>2</sup>·K (existing state) and 0.122 W/m<sup>2</sup>·K (250 mm of EPS).

Three separate cases are investigated with respect to the examined building's envelope. Thus, external walls' U-value might differ from case to case, as shown in Table 4.

- Existing state: existing uninsulated building.
- Conventional renovation: external installation of expanded polystyrene insulation (EPS) with varying thicknesses depending on each scenario.
- Renovation with active layer system add-on component: scenario including the studied solar-driven façade active layer system, where both the active layer and the supply system are installed in addition to the conventionally refurbished building (scenario 2).

Each envelope scenario is coupled with a primary system for heating and cooling. Namely, a natural gas boiler with 80% total efficiency is used for heating, whilst a split air-conditioning unit with EER = 3 is used for cooling. Domestic hot water (DHW) use is partially covered by the natural gas boiler, whereas a 70% contribution from solar collectors has been assumed.

### 3.3. Parametric Study

The parametric study is based on the simulation of 3226 scenarios—combinations of varying design parameters—for each assigned location (Kastoria and Berlin). The analysis takes into account four design parameters, which are listed in Table 5.

**Table 5.** Design parameters of the active layer system.

Parameters		Range	Step
Inlet Temperature	T <sub>in</sub>	19–25 and 26–40 [°C]	1 and 2 [°C] <sup>1</sup>
Solar collector area	A <sub>col</sub>	10–70 [m <sup>2</sup> ]	10 [m <sup>2</sup> ]
Buffer tank volume	V <sub>tank</sub>	0.25–2 [m <sup>3</sup> ]	0.25 [m <sup>3</sup> ]
Insulation thickness	D <sub>ins</sub>	70–100 and 100–250 [mm]	30 and 50 [mm] <sup>2</sup>

<sup>1</sup> 1 °C and 2 °C steps have been considered for inlet temperature ranges of 19–25 [°C] and 26–40 [°C], respectively; <sup>2</sup> 30 mm and 50 mm steps have been considered for insulation thickness ranges of 70–100 [mm] and 100–250 [mm], respectively.

The selection of the examined parameters and their ranges has been defined based on the available literature in the field regarding state-of-the-art thermal barriers or radiant heating/cooling systems [8]. At the same time, the system's limitations in conjunction with the typically dimensioned components used commercially have been considered. In particular, the inlet water temperature entering the external wall's piping

network is selected in order to cover the range of operation as a thermal barrier or radiant heating [8,11,41–44]. The area of the solar collector has a significant impact on the system's heating capacity operation since it is directly linked to the heat source [43]. The volume of the buffer tank serves as a means of varying heat storage in the form of warm water, triggering the system's capacity to operate at times of low sunlight [45,46]. Increasing insulation thickness diminishes the heat losses from the zones and active layer to the ambient environment [47].

The assessment is based on both energy- and cost-related criteria. For all of the simulated scenarios, the heating demand has been considered in order to quantify the contribution of active layer in the building's energy-saving potential.

Additionally, the Net Present Value (NPV) is the economic indicator used for the economic feasibility analysis. The NPV quantifies the investment's worth throughout the technology's lifetime, discounted to today's value. The parametric study has been based on several assumptions presented in Table 6.

**Table 6.** Techno-economic assumptions.

System Component	Cost	
Storage tank	1600	EUR/m <sup>3</sup>
Solar collector	120/200 <sup>1</sup>	EUR/m <sup>2</sup>
Circulation pump	150	EUR
100 mm insulation	60	EUR/m <sup>2</sup>
Additional insulation	1	EUR/cm
Active layer	25	EUR/m <sup>2</sup>
Gas boiler efficiency (for existing state)	80	%
A/C EER for cooling	3	
Natural gas	0.1	EUR/kWh
Electricity from grid	0.14	EUR/kWh
Interest rate	6	%
Lifetime of the system	25	years

<sup>1</sup> 120 and 200 EUR/m<sup>2</sup> have been considered for simple selective and evacuated tube solar collector, respectively.

To estimate the NPV of each parametric case over a 25-year period, constant costs, interest rate and conditions are assumed. The mitigation of heating demands as a reduction factor of the operational space heating cost can be treated as steady yearly income earned by the system installation. Taking into consideration the initial investment cost (CAPEX) and the cash flow (CF), the NPV can be estimated (Equation (2)). Each annual CF refers to the positive amount from the mitigated heating demand compared to the reference case (gas boiler), reduced by the corresponding operational cost (OPEX). The OPEX includes an additional normalized yearly expenditure for maintaining the hot water tank and the solar collectors (EUR 800 every 8 years) as well as the active layer (EUR 400 every 5 years).

$$NPV = CF \cdot \left( \frac{1 - \left( \frac{1}{1+i} \right)^{N+1}}{1 - \frac{1}{1+i}} \right) - CAPEX \quad (2)$$

where NPV is the Net Present Value of the studied investment in [EUR], CF is the constant yearly cash flow in [EUR], CAPEX is the capital expenditure in [EUR], N is the investigated lifetime of technology in [years] and i is the interest rate [%].

Finally, the potential for the simulated case study to reach an nZEB state is also examined. The demand for cooling and domestic hot water are not included in the simulation framework. However, typical values from the TABULA database, with respect to the examined building typology, have been taken into account for the calculation of the cooling and DHW energy demand and the primary energy consumption. Primary energy consumption calculation derives from the energy consumption for heating, cooling and DHW multiplied by the primary energy factors for each fuel used. In our case, the primary energy factor for



electricity is 2.5, as proposed by current EU legislation, whereas, for natural gas, it is 1.1. According to Greek regulations—KENAK (based on the calculation method of the building energy demand according to EN 13790) [41]—the nZEB limit for the renovated state of such a building can rise up to  $71 \frac{\text{kWh}}{\text{m}^2 \cdot \text{a}}$  below  $65 \frac{\text{kWh}}{\text{m}^2 \cdot \text{a}}$  [48].

#### 4. Results

The optimal design of the active layer system for each location is slightly differentiated with respect to the examined parameters. Table 7 presents the techno-economically optimized combinations. The volume of the buffer tank ( $V_{\text{tank}}$ ) and the inlet temperature ( $T_{\text{in}}$ ) are similar for both examined cases. The area of the solar collector ( $A_{\text{col}}$ ) needed in Germany is larger to better support the operation of the active layer system, compared to the Greek case where solar radiation is more exploitable. The suitable insulation thickness ( $D_{\text{ins}}$ ) is 200 mm and 150 mm for the Berlin and Kastoria case, respectively, a fact which indicates the different heating intensities of the two climates.

**Table 7.** Optimal combination of design parameters for each examined location.

Location	$A_{\text{col}}$ (m <sup>2</sup> )	$V_{\text{tank}}$ (m <sup>3</sup> )	$T_{\text{in}}$ (°C)	$D_{\text{ins}}$ (mm)	Heating Demand (kWh/m <sup>2</sup> /Year)
Germany (Berlin)	30	0.25	40	200	21.8
Greece (Kastoria)	20	0.25	40	150	12

Compared to the reference (existing state) scenarios, the optimized design can contribute to a reduction of approximately 82% and 86% for the German and the Greek case, respectively. Figure 5 demonstrates the impact that the application of the active layer system has on the energy needed for heating when operating as a thermal barrier or as a radiant heating system. Specifically, for all simulated scenarios, the highest savings are achieved when the active layer system is used for radiant heating, namely, an 82 and 108 kWh/m<sup>2</sup> heating energy reduction for Kastoria and Berlin, respectively. Operating as a thermal barrier, the potential annual savings are slightly lower, ranging from approximately 60 to 101 kWh/m<sup>2</sup> overall.

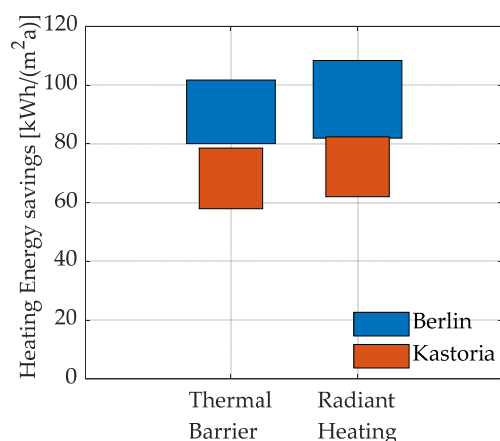


**Figure 5.** Energy savings incurred, reducing heat demand due to the active layer application.

##### 4.1. Techno-Economic/Parametric Study

The results from the parametric analysis form a representative behavior map in terms of sizing of the system's major components, achieved energy savings and feasibility performance. To better understand the overall behavior of the active layer system, it is crucial to deduce how each parameter affects the system's efficiency.

Figure 6 demonstrates the energy demand (a) or the NPV (b) (y-axis) related to the inlet water temperature (x-axis) of the Berlin case. Different color curves represent different collector areas while the dashed lines refer to a tank volume of 1.5 m<sup>3</sup> and the solid lines

to the smallest tank investigated ( $0.25 \text{ m}^3$ ). The variation of insulation thickness does not significantly affect the rest of the parameters; thus, fixed thermal insulation of 20 cm is assumed to facilitate inference. Similar outcomes are also provided for the Kastoria case.

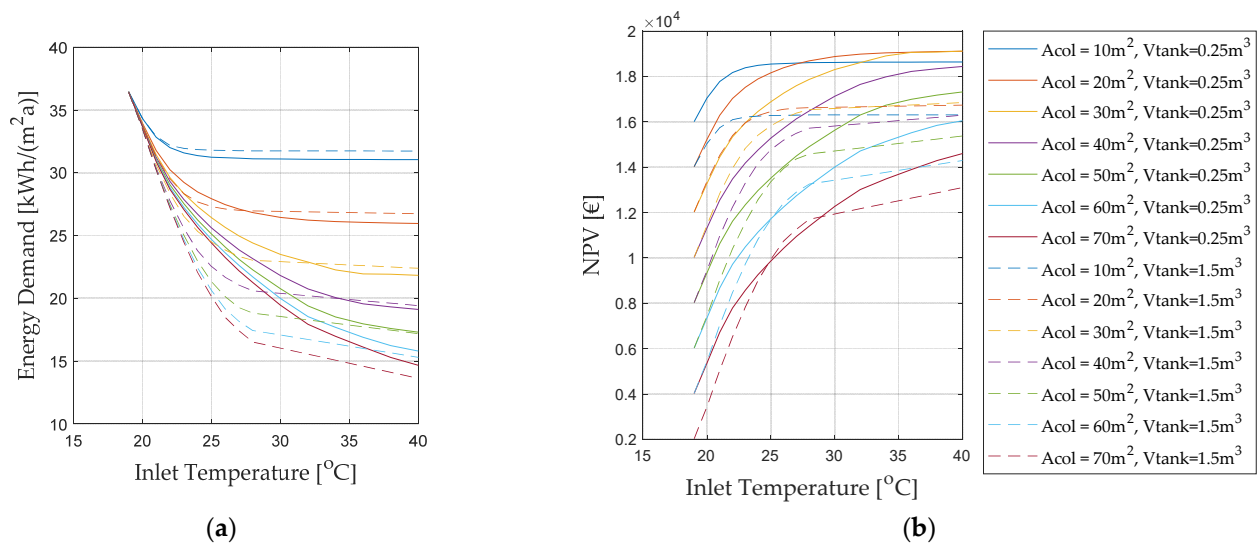


**Figure 6.** Inlet temperature, area of collector and tank volume energy demand (a) and NPV (b) map—Berlin case.

It is clearly shown that higher inlet temperature mitigates the demand for heating. Similarly, wider collector areas lead to higher heat generation and, thus, less energy demands. The smaller collector areas examined, on the other hand, lead the system to reach its capacity limit; thus, further increasing the inlet temperature does not offer further energy savings.

From a techno-economic point of view, the results are significantly more complex and competitive. In particular, smaller collector areas offer relatively higher NPV at low inlet temperatures ( $T_{in}$ ), while bigger areas perform better at higher  $T_{in}$ . Yet, a variety of collector areas lead to high NPV within a narrow range, meaning that the best techno-economic scenario (here  $30 \text{ m}^2$ ) is highly sensitive and may change for different applications or assumptions. Despite the fact that larger solar thermal panels contribute to a more significant decrease in heating demand, this does not necessarily correspond to higher NPV values. Overall, since the heat source is renewable, the increase in  $T_{in}$  is fuel-free, and higher NPV values occur from the mid-range to lower energy demand scenarios. However, the increase in inlet temperature does not practically affect the results indefinitely.

The analysis regarding the tank volume indicates that for low temperatures, higher energy savings can be achieved by bigger tanks. In this case, tank capacity enables storing excess solar energy, leading to further energy demand reduction. In contrast, for relatively high temperatures, the tank volume impact fades away until it is practically insignificant. Namely, as the heat source capacity limit is reached, the need for energy storage vanishes, and thus bigger tanks are not beneficial. On the other hand, it is deduced (Figure 6b) that savings due to larger tank sizes fail to counterbalance the investment cost since smaller tanks offer higher NPV.

Focusing on the impact of the surface area of the collector on NPV with respect to the insulation thickness of the external wall (Figure 7), the trend shows a significant alteration when the water in the active layer system is supplied by a  $30 \text{ m}^2$  area collector. The optimal insulation thickness for two inlet temperatures (25 and  $40 \text{ }^\circ\text{C}$ ) presented is 200 mm, which is expected considering that the simulation refers to the Berlin location, where the demand for heating is significant. When the water temperature entering the active layer is  $25 \text{ }^\circ\text{C}$  (dashed curves), the NPV decreases, proving that for lower inlet temperatures, the area of the solar collector should not exceed  $20 \text{ m}^2$ .

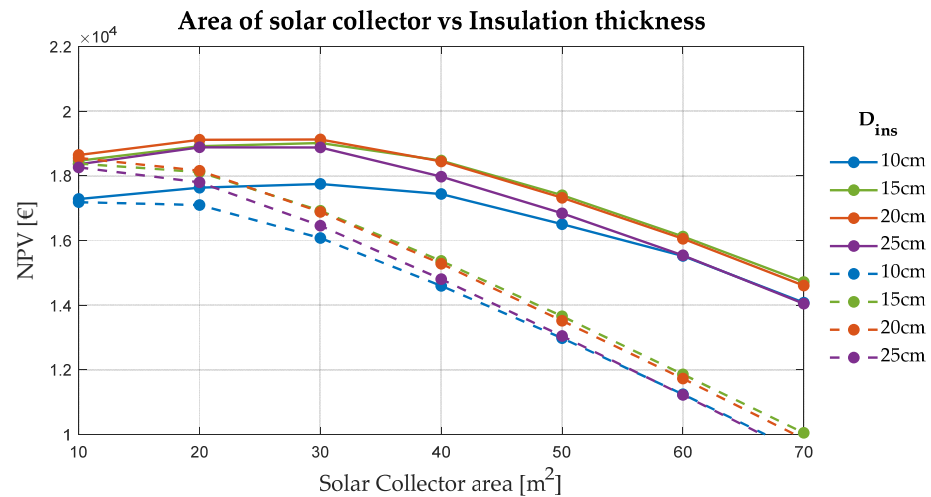


**Figure 7.** NPV taking into account solar collector area and insulation thickness for  $V_{\text{tank}} = 0.25$  and  $T_{\text{in}} = 40\text{ }^{\circ}\text{C}$  (continuous lines) and  $T_{\text{in}} = 25\text{ }^{\circ}\text{C}$  (dashed lines).

As aforementioned, the most critical parameter that characterizes the operation of the active layer is the inlet temperature of the fluid. In cases where the circulating water enters the active layer with an increased temperature of more than  $25\text{ }^{\circ}\text{C}$  [24], the active insulation role of the wall significantly alternates to active heating. Figure 8 presents NPVs correlating to the inlet temperature ( $T_{\text{in}}$ ) with the solar collector area ( $A_{\text{col}}$ ). As an example, for the scenario with a  $10\text{ m}^2$  collector surface, it is observed that when the temperature entering the wall through the active layer is over 25 degrees, the NPV is nearly stabilized. Moreover, it indicates that  $10\text{ m}^2$  area is adequate to support a thermal barrier operation. The lower curves of 40, 50, 60 and  $70\text{ m}^2$  collector area point out that a larger solar collector area, combined with increased inlet temperature, provides the system with higher solar capacity so that the thermostat can be followed. Otherwise, for smaller collector areas, the space heating operation can hardly be achieved.

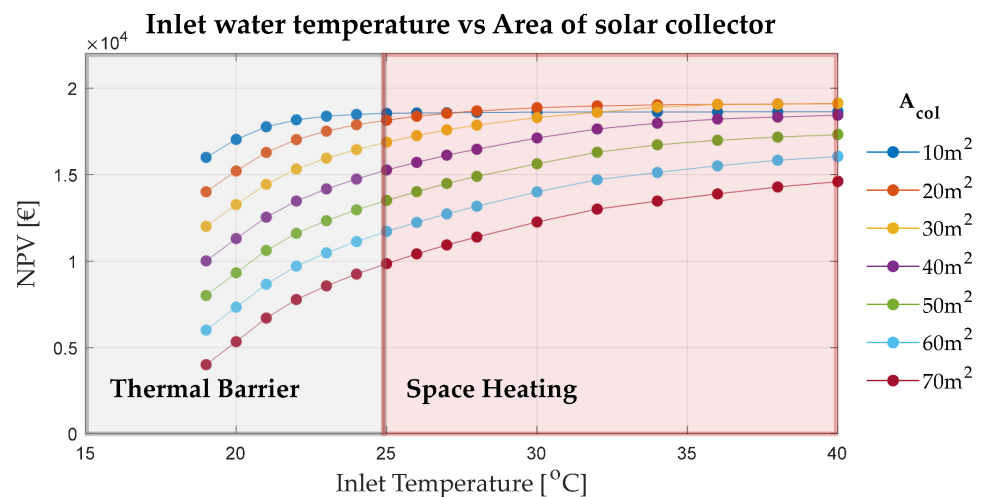


**Figure 8.** Inlet temperature vs. NPV for different collector areas using  $V_{\text{tank}} = 0.25\text{ m}^3$  and  $D_{\text{ins}} = 20\text{ cm}$ .

Assembling the optimal design parameters with respect to their NPV simulated scenarios in the Berlin case (similar trends with lower NPV values are observed for Kastoria), the results depicted in Figure 9 were yielded. Each point (yellow dot) on the surface represents the optimal NPV for each achieved heating demand. The dark red areas in the upper left corner demonstrate the most profitable cases, whereas the green zone corresponds to the techno-economically worst scenarios. The upper surface illustrates the outcome of  $0.25\text{ m}^3$  buffer volume, and the lower surface depicts the results using a tank of  $2\text{ m}^3$ . An insulation

thickness of 200 mm has been considered to be the optimal combination with the active layer system. Both scatter trends are very similar, while the smaller tank scenarios present apparently higher profits. For both of the examined buffer volumes, the NPV values above EUR 18,000 are mainly positioned within the area where the inlet temperature ranges between 36 and 40 °C and the solar collector area ranges between 20 and 30 m<sup>2</sup>. Thus, it is necessary to isolate some of the most characteristic scenarios where the renovation with the investigated technology is considered viable and efficient.

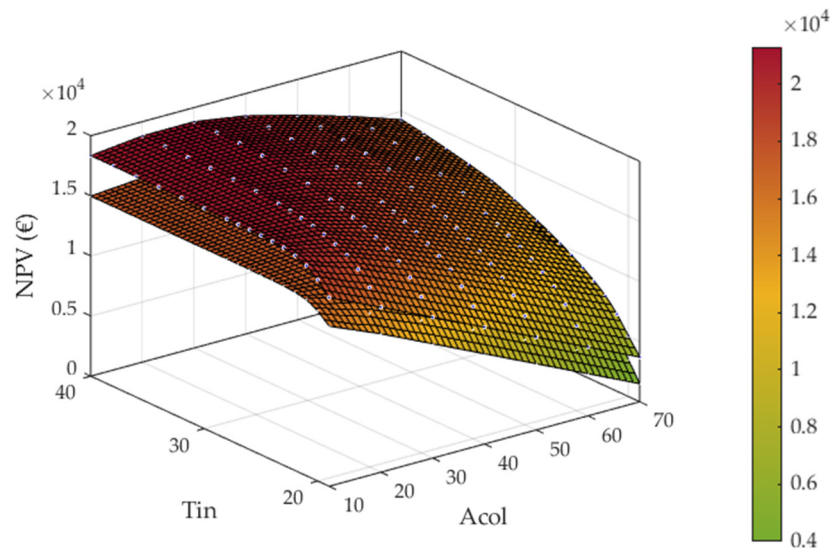


Figure 9. Techno-economically optimal aggregated scenarios.

4.2. Sensitivity Analysis

Following the techno-economic analysis, the impact of financial parameters, such as the interest rate, the investment cost of the active layer’s installation and the solar collector are examined, taking into account the case of the Berlin building. Based on the mapping of the NPV for each simulated case (Figure 9), the optimal cases for each achieved heating demand are scattered, forming a curve, as depicted in Figures 10 and 11. The curves that occurred for each examined financial parameter (interest rate, solar collector cost and active layer cost) are presented with different colors, while each optimal case (points on the curve) is colored according to the corresponding investment cost for each renovation solution.

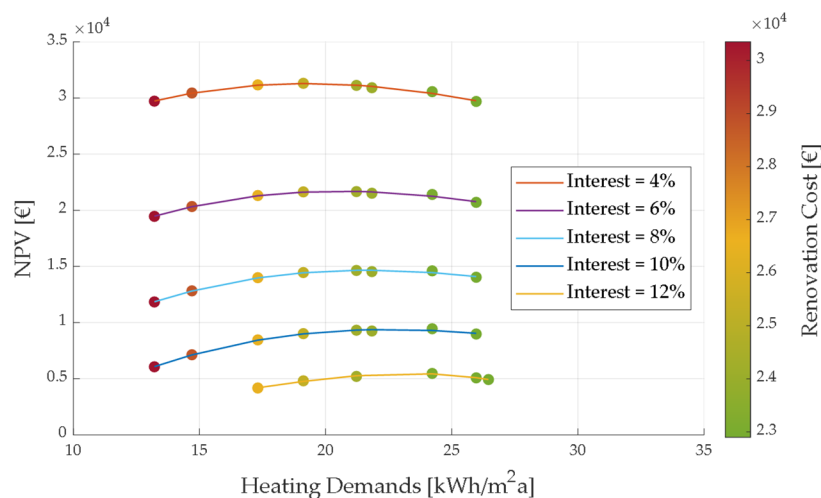
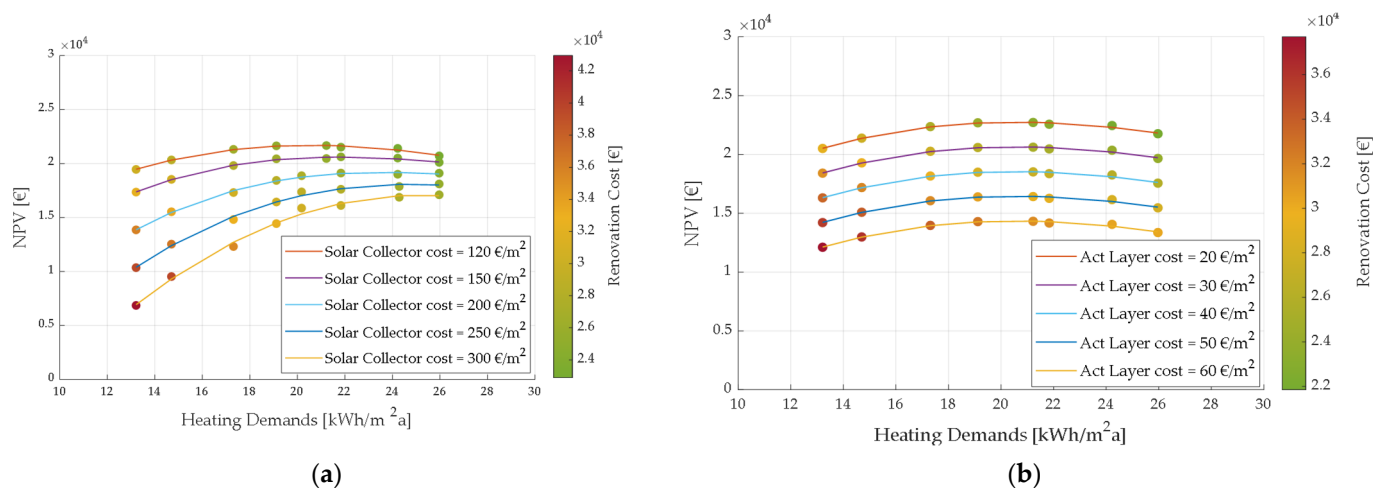


Figure 10. The sensitivity of Pareto curve to the interest rate.



**Figure 11.** The sensitivity of Pareto curve to: (a) solar collector cost and (b) active layer installation cost.

Figure 10 shows the sensitivity of the optimal solutions with respect to different interest rates. Initially, an increment of the interest rate has the opposite impact on the NPV, as expected. Higher renovation cost values lead to the lowest potential heating demand for each interest rate, yet not the most profitable ones. In the scenarios of lower interest rates (i.e., 4%), the increased investment hardly leads to higher NPV. Namely, EUR 30,000 or EUR 23,000 in renovation cost corresponds to a similar NPV of approximately EUR 30,000. On the other hand, the NPV difference considering a 10% interest rate is ca. EUR 3000.

Accordingly, Figure 11 indicates the techno-economic impact of the cost of the active layer system. Specifically, the cost of the solar collector, which is the “heat generator” of the system (a), and the installation of the active layer (b), have been considered. This sensitivity analysis is helpful since the analysis includes two locations—Greece and Germany—with different socio-economic conditions, where such costs may vary significantly. Moreover, the potential of using a more sophisticated and, therefore, more expensive solar collector (evacuated tubes instead of simple collector) can be covered in this analysis. By increasing both the cost of the solar panel and the active layer, unavoidably, the NPV decreases. Furthermore, the cost of the collector seems to be less significant in the cases where the investment cost is minimized. This is due to the fact that these scenarios with the highest heating demand correspond to a smaller area (20 m<sup>2</sup>) of solar collectors.

#### 4.3. Energy Results—nZEB Compliance

It is always useful to compare the energy behavior in the renovated scenario with the existing state since the impact of the renovation solution and the overall savings can be quantified. An additional scenario of typical refurbishment is considered, where conventional thermal insulation (EPS) is added externally to the building’s envelope. Since the analysis focuses on the mitigation of the heating demand, the energy usage for cooling and DHW has not been included in the current study.

Figures 12 and 13 demonstrate the comparison of the existing state of the examined building with the conventionally insulated state and the optimal active layer cases, considering the NPV and the energy demand, respectively. Compared to the existing state of the Greek case, the reduction in heating energy use is 73% for the conventionally insulated scenario, 86% for the NPV-optimal active layer scenario and approximately 93% for the energy-optimal active layer case (considering the cases with 150 mm of insulation). Overall, the corresponding reduction in terms of total primary energy is 50% for the typically insulated scenario, 60% for the most economically feasible active layer case and 67% for the most efficient case.

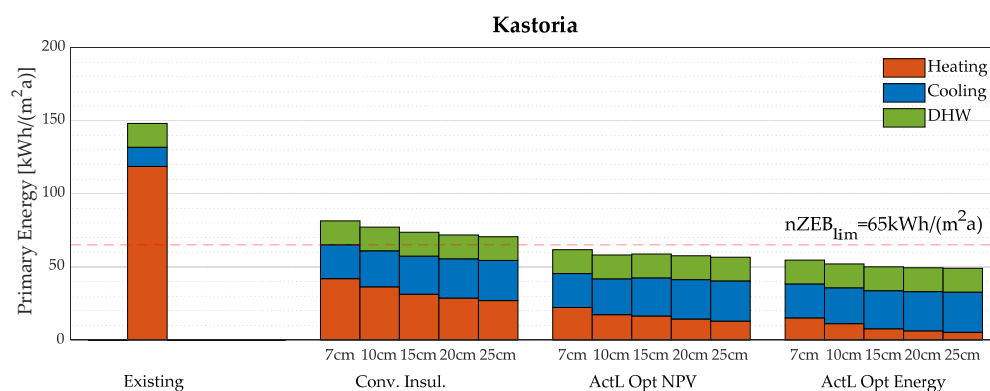


Figure 12. nZEB state compliance for Kastoria case.

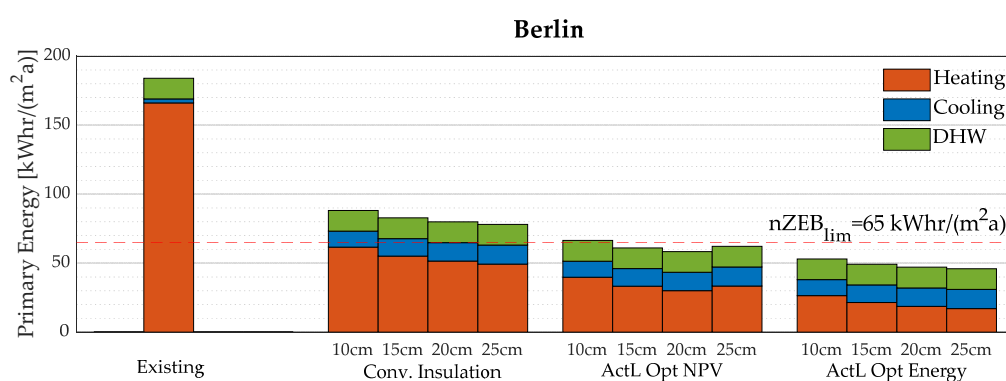


Figure 13. nZEB state compliance in Berlin case.

The application of the active layer system in the German case presents similar results. Comparing the existing (uninsulated) scenario with the optimal active layer case, when considering the NPV, the energy used for heating is reduced by 82%. The active layer system combined with an insulation thickness of 250 mm can mitigate the heating demand (from 166 kWh/m<sup>2</sup> to 17.1 kWh/m<sup>2</sup>). Overall, the primary energy is mitigated by 56% for the conventionally insulated case, 68% for the NPV optimal active layer and 74% for the energy-optimal active layer case.

Accepting the nZEB limitation of 65 kWh/m<sup>2</sup> for both cases, as showcased in Figure 13, an nZEB state is achieved with every techno-economically optimal active layer refurbishment. The results are even better for the optimal cases in terms of energy demand. On the other hand, the scenarios where the building is conventionally insulated fail to comply with the nZEB levels. Taking into account the Greek regulation limitation of 71 kWh/m<sup>2</sup> for refurbished buildings, the case with 25 cm of EPS insulation marginally reaches the nZEB state.

Since passive house (PH) renovation strategies are popular in Germany, a comparison of the Berlin case with PH standards can be useful (Table 8). According to the International Passive House Association (iPHA), a building qualifies for a PH certification in one out of three classes: Classic, Plus and Premium [49]. Each and every PH must comply with various requirements regarding energy demands, construction materials and airtightness. The difference between the Classic, Plus and Premium classes lies in needing less renewable energy demand and simultaneously generating more renewable energy as a surplus.

**Table 8.** Main standards for classic passive house certification.

Criteria		Requirements ( $\leq$ )	Fulfilled?
Space Heating	Heating Demand	$\leq 15 \text{ kWh}/(\text{m}^2\text{a})$	Conditionally Yes
	Heating Load	$\leq 10 \text{ W}/\text{m}^2$	
Primary Energy <sup>1</sup>		$\leq 120 \text{ kWh}/(\text{m}^2\text{a})$	
Airtightness		$0.6 \text{ h}^{-1}$	Yes
Renewable Primary Energy	Demand	$\leq 60 \text{ kWh}/(\text{m}^2\text{a})$	Yes
	Generation	-	-

<sup>1</sup> Includes primary energy need for space heating, cooling/dehumidification (if needed), DHW, lighting, electrical appliances, auxiliary electricity.

As expected, the active layer renovated building is not able to match the PH standards for every parametric combination. Still, in cases where the energy needs are minimized (e.g., Figure 13), such as those of external insulation thicker than 150 mm, the heating demand limit can be reached. The remaining requirements are met for almost every case (see Table 9).

**Table 9.** Minimum criteria for different passive house classes.

Criteria	Classic	Plus	Premium	
Renewable Primary Energy	Demand	$\leq 60 \text{ kWh}/(\text{m}^2\text{a})$	$\leq 45 \text{ kWh}/(\text{m}^2\text{a})$	$\leq 30 \text{ kWh}/(\text{m}^2\text{a})$
	Generation	-	$\geq 60 \text{ kWh}/(\text{m}^2_{\text{ground}}\text{a})$	$\geq 120 \text{ kWh}/(\text{m}^2_{\text{ground}}\text{a})$

Compared to passive house renovation strategies, active layer installation is adequate in terms of meeting the energy standards of a PH. Since even residential passive houses are supposed to be equipped with a heat recovery ventilation unit, the active layer should be combined with a mechanical ventilation system in order to be certificated as a PH. If an additional system, such as photovoltaics, is added for renewable energy generation, the Plus or even Premium class can also be reached.

## 5. Discussion—Conclusions

In the present study, a parametric analysis of a system with a façade-embedded active layer has been conducted in terms of energy and techno-economic criteria in two different climatic conditions (Greece and Germany). Initially, the design parameters have been determined with the aim of optimizing the impact on the heating system. Techno-economic, followed by sensitivity analysis, has been conducted to scrutinize the feasibility of such a renovation solution. Last but not least, the nZEB compliance for both cases has been examined based on EU and national nZEB definitions.

Based on the parametric study, the ideal design of the examined solar-driven system consists of a  $0.25 \text{ m}^3$  volume buffer tank and a  $40 \text{ }^\circ\text{C}$  inlet temperature for the water entering the active layer. These parameters have commonly been proven to be optimal for both climatic conditions. The suitable area of solar panels to support the system is  $20 \text{ m}^2$  for the Greek and  $30 \text{ m}^2$  for the German case. Although evacuated tube panels were used in Berlin, which are more efficient than the simple selective ones used in Kastoria, the solar surface needed is higher to counterbalance the relatively low availability of solar radiation. Moreover, the external side of the active layer should be enhanced by 150 mm and 200 mm of insulation for the Greek and German cases, respectively, highlighting the difference in terms of the space heating intensities of the two examined locations.

Focusing on the inlet temperature of the water, the results of the study indicate the significant effectiveness of the active layer regardless of its operation as a thermal barrier or as a radiant heating system. Comparing two operations in the German climate and considering  $25 \text{ }^\circ\text{C}$  as the marginal setpoint of inlet temperature, the examined system con-

tributes to up to 6.5% more as radiant heating to the heating energy savings. Furthermore, from a techno-economic point of view, the performance of radiant heating was 10% more profitable than operating as dynamic insulation.

In both examined locations, the active layer application is profitable. However, an investment in Berlin proved to be more attractive compared to the case in Kastoria. Even though the available solar radiation is higher in the Mediterranean climate, the heating demands are even lower. Thus, higher energy demand indicates higher potential savings.

It is worth mentioning that such a system can prove extremely useful in cases of geometrical restrictions. When it comes to energy-saving potential over layer thickness, the hydronic system is way more efficient than conventional insulation materials. Indicatively, the thicker conventional insulation examined leads to higher heating demand compared to the active layer enhanced with 70 or 100 mm of additional insulation for the Greek and the German case, respectively. The insulation thickness equivalence that the operation of such an active layer could counterbalance would be a stimulus topic for future work.

Overall, solar-driven façade active layer systems proved to be an effective renovation solution when heating demand requires room for improvement due to its high heating demand reduction capability. Even more, taking into consideration that a single retrofitting intervention can solely contribute to the nZEB state. However, a holistic approach can include the impact of such a system on the energy use for DHW and cooling, which has not been included in this study. In the Greek case, for instance, cooling demand could be tackled significantly by circulating the water between the north and the southern side of the envelope, as proposed in [17,22,23]. Alternatively, a hybrid system of an active layer connected to solar collectors and a (ground source) heat pump could also be further explored [11,12]. However, adding a cooling mode in such a system may increase the risk of condensation effects internally in relation to the wall and additional maintenance and failure costs should be taken into consideration in cases where life cycle analysis should be conducted.

**Author Contributions:** Conceptualization, E.K., P.A.G., I.A., I.M. and M.F.; methodology, E.K., P.A.G., I.A. and I.M.; software, E.K. and P.A.G.; validation, E.K., P.A.G. and I.A.; formal analysis, E.K. and P.A.G.; investigation, E.K. and P.A.G.; resources, M.F.; writing—original draft preparation, E.K.; writing—review and editing, I.A. and I.M.; visualization, I.A.; supervision, M.F.; project administration, M.F.; funding acquisition, M.F. All authors have read and agreed to the published version of the manuscript.

**Funding:** This research was funded by the Horizon 2020 European Research & Innovation project PLURAL: “Plug-and-use renovation with adaptable lightweight systems”, grant number 958218.

**Data Availability Statement:** Data are not available due to privacy restrictions.

**Conflicts of Interest:** The authors declare no conflict of interest. The funders had no role in the design of the study; in the collection, analyses, or interpretation of data; in the writing of the manuscript; or in the decision to publish the results.

## References

1. D’Agostino, D.; Tzeiranaki, S.T.; Zangheri, P.; Bertoldi, P. Assessing Nearly Zero Energy Buildings (NZEBS) Development in Europe. *Energy Strategy Rev.* **2021**, *36*, 100680. [[CrossRef](#)]
2. Daouas, N. A Study on Optimum Insulation Thickness in Walls and Energy Savings in Tunisian Buildings Based on Analytical Calculation of Cooling and Heating Transmission Loads. *Appl. Energy* **2011**, *88*, 156–164. [[CrossRef](#)]
3. Alayed, E.; Bensaid, D.; O’Hegarty, R.; Kinnane, O. Thermal Mass Impact on Energy Consumption for Buildings in Hot Climates: A Novel Finite Element Modelling Study Comparing Building Constructions for Arid Climates in Saudi Arabia. *Energy Build.* **2022**, *271*, 112324. [[CrossRef](#)]
4. Imbabi, M.S.E. A Passive–Active Dynamic Insulation System for All Climates. *Int. J. Sustain. Built Environ.* **2012**, *1*, 247–258. [[CrossRef](#)]
5. Kotsiris, G.; Androutopoulos, A.; Polychroni, E.; Nektarios, P.A. Dynamic U-Value Estimation and Energy Simulation for Green Roofs. *Energy Build.* **2012**, *45*, 240–249. [[CrossRef](#)]
6. Pihelo, P.; Kuusk, K.; Kalamees, T. Development and Performance Assessment of Prefabricated Insulation Elements for Deep Energy Renovation of Apartment Buildings. *Energies* **2020**, *13*, 1709. [[CrossRef](#)]



7. Bigaila, E.; Athienitis, A.K. Modeling and Simulation of a Photovoltaic/Thermal Air Collector Assisting a Façade Integrated Small Scale Heat Pump with Radiant PCM Panel. *Energy Build.* **2017**, *149*, 298–309. [[CrossRef](#)]
8. Krajčák, M.; Arıcı, M.; Šikula, O.; Šimko, M. Review of Water-Based Wall Systems: Heating, Cooling, and Thermal Barriers. *Energy Build.* **2021**, *253*, 111476. [[CrossRef](#)]
9. ASHRAE. *Handbook HVAC Systems and Equipment*; American Society of Heating, Refrigerating and Air-Conditioning Engineers, Inc.: Atlanta, GA, USA, 2012.
10. Babiak, J.; Olesen, B.W.; Petras, D. *REHVA Guidebook No 7: Low Temperature Heating and High Temperature Cooling*, 1st ed.; Federation of European Heating and Air-Conditioning Associations: Brussels, Belgium, 2009.
11. Karmann, C.; Schiavon, S.; Bauman, F. Thermal Comfort in Buildings Using Radiant vs. All-Air Systems: A Critical Literature Review. *Build. Environ.* **2017**, *111*, 123–131. [[CrossRef](#)]
12. Romani, J.; Pérez, G.; de Gracia, A. Experimental Evaluation of a Heating Radiant Wall Coupled to a Ground Source Heat Pump. *Renew. Energy* **2017**, *105*, 520–529. [[CrossRef](#)]
13. Krajčák, M.; Šikula, O. The Possibilities and Limitations of Using Radiant Wall Cooling in New and Retrofitted Existing Buildings. *Appl. Therm. Eng.* **2020**, *164*, 114490. [[CrossRef](#)]
14. Oravec, J.; Šikula, O.; Krajčák, M.; Arıcı, M.; Mohapl, M. A Comparative Study on the Applicability of Six Radiant Floor, Wall, and Ceiling Heating Systems Based on Thermal Performance Analysis. *J. Build. Eng.* **2021**, *36*, 102133. [[CrossRef](#)]
15. Mikeska, T.; Svendsen, S. Dynamic Behavior of Radiant Cooling System Based on Capillary Tubes in Walls Made of High Performance Concrete. *Energy Build.* **2015**, *108*, 92–100. [[CrossRef](#)]
16. Šimko, M.; Krajčák, M.; Šikula, O.; Šimko, P.; Kalús, D. Insulation Panels for Active Control of Heat Transfer in Walls Operated as Space Heating or as a Thermal Barrier: Numerical Simulations and Experiments. *Energy Build.* **2018**, *158*, 135–146. [[CrossRef](#)]
17. Shen, J.; Wang, Z.; Luo, Y.; Jiang, X.; Zhao, H.; Cui, D.; Tian, Z. Performance Evaluation of an Active Pipe-Embedded Building Envelope System to Transfer Solar Heat Gain from the South to the North External Wall. *J. Build. Eng.* **2022**, *59*, 105123. [[CrossRef](#)]
18. Zhou, L.; Li, C. Study on Thermal and Energy-Saving Performances of Pipe-Embedded Wall Utilizing Low-Grade Energy. *Appl. Therm. Eng.* **2020**, *176*, 115477. [[CrossRef](#)]
19. Krzaczek, M.; Kowalczyk, Z. Thermal Barrier as a Technique of Indirect Heating and Cooling for Residential Buildings. *Energy Build.* **2011**, *43*, 823–837. [[CrossRef](#)]
20. Ma, P.; Wang, L.S.; Guo, N. Energy Storage and Heat Extraction—From Thermally Activated Building Systems (TABS) to Thermally Homeostatic Buildings. *Renew. Sustain. Energy Rev.* **2015**, *45*, 677–685. [[CrossRef](#)]
21. Yu, Y.; Niu, F.; Guo, H.A.; Woradachjumnroen, D. A Thermo-Activated Wall for Load Reduction and Supplementary Cooling with Free to Low-Cost Thermal Water. *Energy* **2016**, *99*, 250–265. [[CrossRef](#)]
22. Ibrahim, M.; Wurtz, E.; Anger, J.; Ibrahim, O. Experimental and Numerical Study on a Novel Low Temperature Façade Solar Thermal Collector to Decrease the Heating Demands: A South-North Pipe-Embedded Closed-Water-Loop System. *Sol. Energy* **2017**, *147*, 22–36. [[CrossRef](#)]
23. Ibrahim, M.; Wurtz, E.; Biwole, P.H.; Achard, P. Transferring the South Solar Energy to the North Façade through Embedded Water Pipes. *Energy* **2014**, *78*, 834–845. [[CrossRef](#)]
24. Kisilewicz, T.; Fedorczyk-Cisak, M.; Barkanyi, T. Active Thermal Insulation as an Element Limiting Heat Loss through External Walls. *Energy Build.* **2019**, *205*, 109541. [[CrossRef](#)]
25. Zhu, Q.; Li, A.; Xie, J.; Li, W.; Xu, X. Experimental Validation of a Semi-Dynamic Simplified Model of Active Pipe-Embedded Building Envelope. *Int. J. Therm. Sci.* **2016**, *108*, 70–80. [[CrossRef](#)]
26. Iffa, E.; Hun, D.; Salonvaara, M.; Shrestha, S.; Lapsa, M. Performance Evaluation of a Dynamic Wall Integrated with Active Insulation and Thermal Energy Storage Systems. *J. Energy Storage* **2022**, *46*, 103815. [[CrossRef](#)]
27. Lehmann, B.; Dorer, V.; Koschenz, M. Application Range of Thermally Activated Building Systems Tabs. *Energy Build.* **2007**, *39*, 593–598. [[CrossRef](#)]
28. Gwerder, M.; Lehmann, B.; Tödtli, J.; Dorer, V.; Renggli, F. Control of Thermally-Activated Building Systems (TABS). *Appl. Energy* **2008**, *85*, 565–581. [[CrossRef](#)]
29. Olsthoorn, D.; Haghighat, F.; Moreau, A.; Lacroix, G. Abilities and Limitations of Thermal Mass Activation for Thermal Comfort, Peak Shifting and Shaving: A Review. *Build. Environ.* **2017**, *118*, 113–127. [[CrossRef](#)]
30. Schmelas, M.; Feldmann, T.; Bollin, E. Savings through the Use of Adaptive Predictive Control of Thermo-Active Building Systems (TABS): A Case Study. *Appl. Energy* **2017**, *199*, 294–309. [[CrossRef](#)]
31. Aste, N.; Leonforte, F.; Manfren, M.; Mazzon, M. Thermal Inertia and Energy Efficiency—Parametric Simulation Assessment on a Calibrated Case Study. *Appl. Energy* **2015**, *145*, 111–123. [[CrossRef](#)]
32. Zhang, Z.; Sun, Z.; Duan, C. A New Type of Passive Solar Energy Utilization Technology—The Wall Implanted with Heat Pipes. *Energy Build.* **2014**, *84*, 111–116. [[CrossRef](#)]
33. Barzin, R.; Chen, J.J.; Young, B.R.; Farid, M.M. Application of PCM Underfloor Heating in Combination with PCM Wallboards for Space Heating Using Price Based Control System. *Appl. Energy* **2015**, *148*, 39–48. [[CrossRef](#)]
34. Li, A.; Xu, X.; Sun, Y. A Study on Pipe-Embedded Wall Integrated with Ground Source-Coupled Heat Exchanger for Enhanced Building Energy Efficiency in Diverse Climate Regions. *Energy Build.* **2016**, *121*, 139–151. [[CrossRef](#)]

35. Antretter, F.; Hun, D.; Boudreaux, P.; Member, A.; Cui, B. Assessing the Potential of Active Insulation Systems to Reduce Energy Consumption and Enhance Electrical Grid Services. In Proceedings of the Conference: 2019 Buildings XIV International Conference, Georgia, FL, USA, 9–12 December 2019.
36. Zavrel, V.; Matuška, T.; Zmrhal, V. Building Energy Modelling for Development of Active Facade Panel with Solar Generation and Thermoelectric Air-Conditioning Unit. In Proceedings of the Building Simulation Conference Proceedings, Rome, Italy, 2–4 September 2019; International Building Performance Simulation Association: Atlanta, GA, USA, 2019; Volume 3, pp. 1824–1831.
37. Keshavarzadeh, A.H.; Ahmadi, P. Multi-Objective Techno-Economic Optimization of a Solar Based Integrated Energy System Using Various Optimization Methods. *Energy Convers. Manag.* **2019**, *196*, 196–210. [[CrossRef](#)]
38. Klein, S.A. *TRNSYS 18: A Transient System Simulation Program*; Aiguasol: Madison, WI, USA, 2018.
39. Loga, T.; Balaras, C.; Dascalaki, E.; Sijanec Zavrl, M.; Rakusek, A.; Corrado, V.; Corgnati, S.; Despretz, H.; Roarty, C.; Hanratty, M.; et al. Use of Building Typologies for Energy Performance Assessment of National Building Stocks Existing Experiences in European Countries and Common Approach. Institut Wohnen und Umwelt GmbH: Darmstadt, Germany, 2010; ISBN 9783941140141.
40. Androutsopoulos, A.; Aravantinos, D.; Gaglia, A.; Giannakidis, G.; Gidakou, G.; Dimoudi, A.; Droutsa, K.; Efthimiadis, A.; Zaharias, P.; Iliadis, G.; et al. Regulation on the Energy Performance of Buildings (KENAK); Greece. 2017. Available online: <http://portal.tee.gr/portal/page/portal/tpree/totee/TOTEE-20701-1-Final-%D4%C5%C5-3rd%20edition.pdf> (accessed on 25 April 2023).
41. Zhou, Y.; Zheng, S.; Chen, H.; Zhang, G. Thermal Performance and Optimized Thickness of Active Shape-Stabilized PCM Boards for Side-Wall Cooling and under-Floor Heating System. *Indoor Built. Environ.* **2016**, *25*, 1279–1295. [[CrossRef](#)]
42. Ning, B.; Schiavon, S.; Bauman, F.S. Topic A4. Advanced or Innovative HVAC&R Systems and System Components A Classification Scheme for Radiant Systems Based on Thermal Time Constant. Available online: <https://escholarship.org/uc/item/1sx88662> (accessed on 25 April 2023).
43. Qiao, X.; Kong, X.; Li, H.; Wang, L.; Long, H. Performance and Optimization of a Novel Active Solar Heating Wall Coupled with Phase Change Material. *J. Clean Prod.* **2020**, *250*, 119470. [[CrossRef](#)]
44. Giovanardi, A.; Passera, A.; Zottele, F.; Lollini, R. Integrated Solar Thermal Façade System for Building Retrofit. *Solar Energy* **2015**, *122*, 1100–1116. [[CrossRef](#)]
45. Li, J.; Li, X.; Wang, Y.; Tu, J. Long-Term Performance of a Solar Water Heating System with a Novel Variable-Volume Tank. *Renew. Energy* **2021**, *164*, 230–241. [[CrossRef](#)]
46. Guo, X.; Shu, H.; Gao, J.; Xu, F.; Cheng, C.; Sun, Z.; Xu, D. Volume Design of the Heat Storage Tank of Solar Assisted Water-Source Heat Pump Space Heating System. In *Proceedings of the Procedia Engineering*; Elsevier Ltd.: Amsterdam, The Netherlands, 2017; Volume 205, pp. 2691–2697.
47. Junasová, B.; Krajčík, M.; Šikula, O.; Arıcı, M.; Šimko, M. Adapting the Construction of Radiant Heating and Cooling Systems for Building Retrofit. *Energy Build.* **2022**, *268*, 112228. [[CrossRef](#)]
48. Dascalaki, E.G.; Balaras, C.A.; Gaglia, A.G.; Droutsa, K.G.; Kontoyiannidis, S. Energy Performance of Buildings-EPBD in Greece. *Energy Policy* **2012**, *45*, 469–477. [[CrossRef](#)]
49. International Passive House Association Passive House Standards. Available online: <https://passivehouse-international.org/index.php> (accessed on 25 April 2023).

**Disclaimer/Publisher’s Note:** The statements, opinions and data contained in all publications are solely those of the individual author(s) and contributor(s) and not of MDPI and/or the editor(s). MDPI and/or the editor(s) disclaim responsibility for any injury to people or property resulting from any ideas, methods, instructions or products referred to in the content.